

Article

# Neural Image Analysis and Electron Microscopy to Detect and Describe Selected Quality Factors of Fruit and Vegetable Spray-Dried Powders—Case Study: Chokeberry Powder

Krzysztof Przybył<sup>1</sup>, Jolanta Gawalek<sup>1</sup>, Krzysztof Koszela<sup>2,\*</sup> , Jacek Przybył<sup>2</sup>,  
Magdalena Rudzińska<sup>1</sup>, Łukasz Gierz<sup>3</sup>  and Ewa Domian<sup>4</sup>

- <sup>1</sup> Food Sciences and Nutrition, Institute of Food Technology of Plant Origin, Poznan University of Life Sciences, Wojska Polskiego 31, 60-624 Poznan, Poland; kprzybyl@up.poznan.pl (K.P.); jolanta.gawalek@up.poznan.pl (J.G.); magdar@up.poznan.pl (M.R.)
- <sup>2</sup> Institute of Biosystems Engineering, Poznan University of Life Sciences, Wojska Polskiego 50, 60-625 Poznan, Poland; jacek.przybyl@up.poznan.pl
- <sup>3</sup> Faculty of Transport Engineering, Poznan University of Technology, 60-624 Poznan, Poland; lukasz.gierz@put.poznan.pl
- <sup>4</sup> Department of Food Engineering and Process Management, Warsaw University of Life Sciences—SGGW, 02-787 Warsaw, Poland; ewa\_domian@sggw.pl
- \* Correspondence: koszela@up.poznan.pl; Tel.: +48-502-288-097

Received: 15 September 2019; Accepted: 8 October 2019; Published: 12 October 2019



**Abstract:** The study concentrates on researching possibilities of using computer image analysis and neural modeling in order to assess selected quality discriminants of spray-dried chokeberry powder. The aim of the paper is the quality identification of chokeberry powders on account of their highest drying power, the highest bioactivity, as well as technologically satisfying looseness of the powder. The article presents neural models with vision techniques backed up by devices such as digital cameras, as well as an electron microscope. The reduction in size of input variables with PCA has an influence on improving the processes of learning data sets, thus increasing the effectiveness of identifying chokeberry fruit powders included in digital pictures, which is shown in the results of the conducted research. The effectiveness of image recognition is presented by classifying abilities, as well as low Root Mean Square Error (RMSE), for which the best results are achieved with a typology of network type Multi-Layer Perceptron (MLP). The selected networks type MLP are characterized by the highest degree of classification at 0.99 and RMSE at 0.11 at most at the same time.

**Keywords:** Artificial Neural Network (ANN); classification; image analysis; chokeberry powder; colors; spray-drying

## 1. Introduction

Chokeberry (*Aronia melanocarpa* L.) is a rich source of valuable nutrients, among other things, vitamins and polyphenols. It is also characterized by a high content of antioxidants, which have a positive influence on improving eyesight as well as lower blood pressure [1,2] and lead to early inhibition of cancerogenic stages [3–5]. The basic antioxidants that can be found in chokeberry fruit are anthocyanins [6]. Anthocyanins are pigments, which give chokeberry fruit a characteristic dark color [7]. Color intensity depends on pH; when pH is low, the color is intensely red; when pH rises, the color changes into dark blue [8]. Chokeberry also contains valuable tannins (tanning agents), which are responsible for its sensory characteristics, giving chokeberry fruit a very characteristic tart taste [9].

On account of that product obtained from chokeberry, including chokeberry powders, are widely used in functional and pro-health food as well as in all food industries as natural red and dark-blue dye. The still increasing customer awareness in recent years in terms of healthy nutrition leads to an increase in demand for food of natural origin characterized by pro-health properties. At the same time, a dynamically developing trend of foodstuffs fast to make at any moment and in any place, determine the development of instant food technology [10]. Dried vegetable products, especially fruit products, are ideal semifinished goods used in the production of this type of food. Fruits could be dried as whole fruits or their particles, pastes, and juices. A very disadvantageous phenomenon regarding dried food products is the shrinkage of dried material, so changes in the shape and texture of the finished dried product are related to the breaking of capillaries during the drying process [11]. In the case of drying paste and fruit juices, the most commonly used method is spray-dried method with carrier five such powders on a large scale is not easy due to their stickiness [12].

These phenomena are linked with a high content of simple sugars and organic acids, which are characterized by the low temperature of verification ( $T_g$ ). During the process of spray-drying, powders of different morphology and particle microstructure are formed [10,13]. It results from different conditions of drying such as the way and conditions of spraying liquid (i.e., rotary atomizer and its rotary speed), inlet temperature of drying air (inlet and outlet air temperature), physicochemical parameters of feed to be dried [13]. One of the examples is increasing the inlet air temperature, which causes an increase in the speed of drying, and at the same time, causes lower shrinking of particles [14]. In consequence, powder particles are characterized by bigger size and other microstructure are formed [15]. When the inlet temperature of the spray-dried powder is low, the majority of particles show withered surfaces while increasing the inlet temperature results in a larger number of particles of smooth surfaces [16]. A different situation occurs when rotary atomizer speed, then there is a tendency to form particles characterized by smaller sizes [17]. The microstructure of powder particles, in turn, has an influence on functional parameters, which directly determine the abilities of their application. Flowability is one of the most important features of powders because it affects the powders' behaviors in various processes, e.g., transport, mixing, and dosage [5]. Parameters which have a substantial influence on powder looseness, among other things, are the particle size distribution, loose bulk density, tapped bulk density, the density of the powder particles, the volume of the interstitial air, moisture [5,18–20]. A particularly important parameter to characterize features of fruit powders on account of packaging processes, transport, and storing is loose and tapped bulk density. Fleck compaction in powder (compressibility) influences bulk density. Loose bulk density is a volume of loosely poured powdered material, while tapped bulk density that is shaken down is a volume of powder compressed in a normalized way (empty volumes between particles are eliminated) [21–23]. Apart from numerous physical features of fruit powders, bioactive features are also crucial, which results from retaining properties of fresh fruit juices from which they are produced. It has an enormous meaning in the application of those powders, as pro-pro-health additives or as natural dyes used in the food and pharmaceutical industry [5,16,20,24]. In industrial production of such powders, a key issue is getting suitable quality, which is determined by given values of various physical and chemical parameters. Marking all parameters in the laboratory is time-consuming; thus a search for fast techniques of assessing the quality of powders during the production process is being continued at all times [10].

In the face of diversity of neural networks resulting from using numerous architectures, a really important stage is the selection of those, which, in an ambiguous way, are able to solve a given problem that is under research. Classification is understood as finding such a classifier, which allows dividing the set of elements into groups, called classes [25–27]. Elements belonging to one group are called objects. There can be differences between them, but not in case of properties, on account of which, they were assigned to a given class. One of the examples of neural networks used most commonly in classification issues is Multi-Layer Perceptron (MLP) [28,29]. It is a unidirectional network using a method of learning with a teacher [30,31], possessing a multi-layer architecture with at least one

hidden layer [10]. The only possible communication is the one between neurons in adjacent layers. The activating function for hidden neurons has a non-linear character (sigmoid character) [32].

The aim of the research was to provide assessment and quality identification of chokeberry powders on the grounds of its dyeing capabilities as well as to gain the highest bioactivity (i.e., the highest content of anthocyanin and the highest value of antioxidant potential). In addition to the above, the quality assessment also included measuring the proper level of powders' looseness (indirectly via microstructure and morphology of particles). In order to achieve this goal, a vision technique with a digital camera was used, using dyeing power on the outer surface as well as electron microscopy using the shapes of the inner structure (morphology structure) of spray-dried chokeberry juices. The utilitarian goal was to devise a neural model capable of classifying research samples of chokeberry powders, which does not stand out from industrial patterns with defined dyeing and bioactive properties and were as looseness properties in terms of color and structure. The authors verified the research results for the formulated neural models. The assessment error called RMS served as a quality indicator of the formulated models. The formulated neural models were characterized by a high degree of accuracy classification. Due to the above, the research aim of the paper was executed.

## 2. Materials and Methods

### 2.1. Preparation of Spray-Dried Chokeberry Powders

Drying was performed using a semi-industrial spray dryer—Niro Atomiser type FU 11 DA (Denmark)—which allowed to perform a full equivalent of the industrial process. Commercial, concentrated chokeberry juice (SVZ International B.V., Holland) (65 Brix) was used in the study. Maltodextrin, with two degrees of crystallization, was used as a carrier DE: 8 and 22 (Roquette Freres—France). The content of all powders that were received was identical: 30% of fruit and 70% of the carrier in dry powder mass. The process was performed for the following inlet air temperature: 150, 160, 170 °C, and with the following values of the rotary atomizer's rotational speed: 12,000, 13,000, 14,000 rpm. Table 1 presents the experimental conditions used for the spray-drying of chokeberry juice with the carrier.

**Table 1.** Experimental conditions used for the spray-drying of chokeberry juice with a carrier.

Powder Code	DE Carrier	Carrier Content (%)	Inlet Air Temperature (°C)	Rotary Atomizer Speed (rpm)
AR_1	8	70	150	12,000
AR_2	8	70	160	12,000
AR_3	8	70	170	12,000
AR_4	8	70	160	13,000
AR_5	8	70	160	14,000
AR_6	22	70	160	12,000

### 2.2. Image Preparation

The study concentrates mainly on the comparative analysis of chokeberry powders received in various variants of spray drying in accordance with Table 1. Different parameters of drying simultaneously determine different functional properties of powders, that is why the 6 test trials were called quality classes (AR\_1, AR\_2, AR\_3, AR\_4, AR\_5, and AR\_6). The first step with a digital camera and site for image acquisition [10] required acquiring colored 24-bit images that have 4928 × 3264 resolution of color space models RGB (Red Green Blue). One of the methods of computer image analysis was used, i.e., segmentation, that allowed receiving 3050 objects in the form of image patterns that had 450 × 450 resolution. Table 2 presents the layout of objects occurring in given classes of spray-dried chokeberry juice.

**Table 2.** Layout of frequency of output variables in training set.

Output Variable	AR_1	AR_2	AR_3	AR_4	AR_5	AR_6	AR_ALL
number of cases regarding color	496	512	426	484	474	658	3050
%	16.26	16.79	13.97	15.87	15.54	21.57	100
number of cases regarding shape	978	1266	1150	1370	1464	1178	7406
%	13.21	17.09	15.53	18.50	19.77	15.91	100

Image histogram was used in the research, which allows characterizing image globally on the basis of encoded numerical data. Parameters determining histogram are measurements and statistics of the image such as average, standard deviation, median, minimum, and maximum. Using the author's original software "PID system", recommended parameters for file (with .csv extension) were extracted, creating the so-called training set [10,33]. The software allows distinguishing recommended features from image included in color space model RGB [34], as well as H\_S\_B\_L (Hue Saturation Brightness Lightness) and YCbCr (Y is luma component and CB and CR are the blue-difference and red-difference chroma components, respectively) [35,36]. The selected model of colors was achieved on the basis of the mathematical conversion of the RGB color. Tables 3 and 4 variable input data present image descriptors determining the aforementioned numerical data, which are encoded in color space models. The procedures of image processing were presented in previous research on strawberry powders [10].

**Table 3.** Results of training process ANN with a selection of all output variables.

Name	MLP 23:23-25-6:1	MLP 10:10-3-6:1
Input variables	RGB, YCbCR, H_S_B_L	shape factors
Output variables	All AR	All AR
Training error	0.1127	0.3695
Validation error	0.1268	0.3703
Testing error	0.1357	0.3706
Quality of training	0.9443	0.2425
Quality of validation	0.9396	0.2366
Quality of testing	0.9253	0.2408
Training algorithm	BP50, CG303b	BP50, CG150b
Learning cases	3050	7406
RMSE	0.1251	0.3701
MSE	0.3537	0.6084
Accuracy	0.9541	0.2371

**Table 4.** Results of training process ANN with the selection of differences in parameters influencing the drying process (inlet air temperature, rotary atomizer speed, as well as the degree of saccharification of the drying carrier (DE)).

Name	MLP 12:12-2-3:1	MLP 15:15-5-3:1	MLP 15:15-25-3:1	MLP 12:12-3-2:1	MLP 15:15-10-2:1
Input variables	RGB	YCbCR	YCbCr	RGB	YCbCr
Output variables	AR_2, AR_4, AR_5	AR_2, AR_4, AR_5	AR_1, AR_2, AR_3	AR_2, AR_6	AR_2, AR_6
Training error	0.1513	0.1132	0.0798	0.0047	0.0312
Validation error	0.1675	0.1292	0.0814	0.0033	0.0573
Testing error	0.1696	0.2008	0.1665	0.0269	0.0646
Quality of training	0.9538	0.9837	0.9916	0.9999	0.9983
Quality of validation	0.9511	0.9674	0.9944	0.9999	0.9966
Quality of testing	0.9399	0.9344	0.9497	0.9999	0.9967
Training algorithm	BP50, CG300b	BP50, CG45b	BP50, CG48b	BP50, CG229b	BP50, CG76b
Learning cases	1470	1470	1434	1170	1170
RMSE	0.1628	0.1477	0.1092	0.0117	0.0510
MSE	0.4035	0.3843	0.3305	0.1082	0.2259
Accuracy	0.9497	0.9673	0.9940	0.9999	0.9999

Within the comparison of the efficiency of recognizing chokeberry powders, digital images with the technique of electron microscopy were used. While the research, fragments of fruit powder were indicated, achieving 24-bit images within a range of grey color that has  $480 \times 390$  resolution. On the basis of 12 images, two from each class of chokeberry powders quality, 7406 micro-particles were marked from an image. Micro-particles were achieved with an electron microscope Hitachi TM3000 Tabletop scanning electron microscope (Hitachi High-Technologies Corp., Tokyo, Japan). The study design of acquiring scanning images was achieved on the basis of the previously conducted research on chokeberry powders [5]. The process of processing scanning images consisted of several stages, whose aim was to create image convolution with a Canny filter [33], making image binarization [33] as well as extracting features of shape coefficient with micro-particles occurring on the image (Figures 1 and 2) [33].

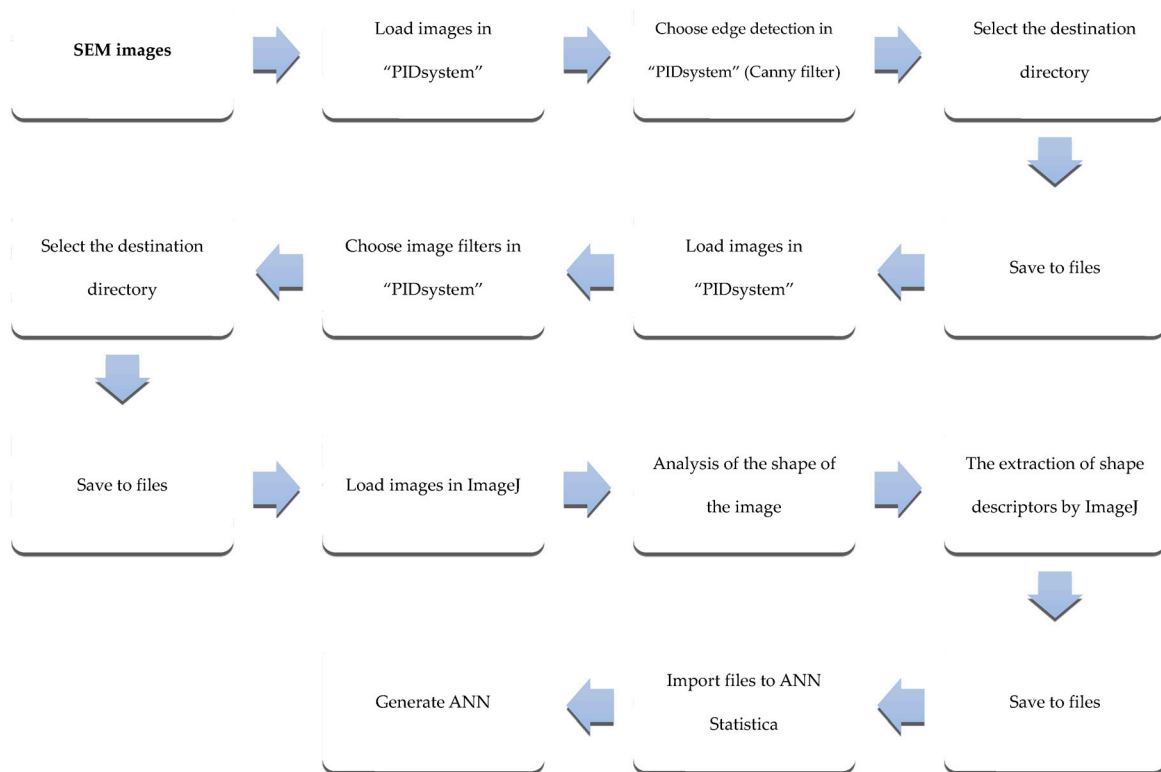


**Figure 1.** Scheme of the procedure to determine the shape factors to obtain a neural model based on scanning electron microscopy (SEM) images.

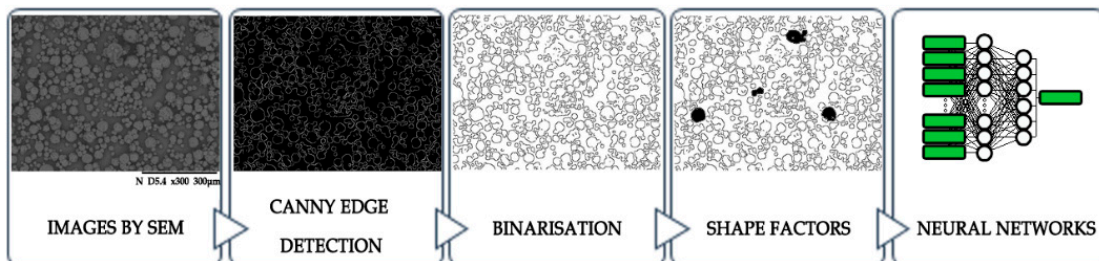


**Figure 2.** Scheme of shape factors which were extracted of image to the learning process of Neural Networks.

### 2.3. Canny Edge Detection

Filter application in image processing is a well-known solution in determining, among other things, edges, pixel weight, noise reduction, removal of granulation, sharpness improvement, changes in recording format, as well as image resolution. The aim is to gain information encoded in the bitmap, as well as determining meaningful image pixels. The Canny method of detection is nothing else but automatic detection of the layout of particle sizes with image analysis based on local adaptive edge detection [37]. The Canny method optimizes three basis criteria: minimizes the number of faulty detections, ensures precise edges localization as well as generates a single answer for each real edge in the image [38].

Edge detection in the image is a popular and effective solution. Among well-known solutions of image convolution, apart from the Canny's, one can also mention, Roberts, Prewitt, Kirsch, Sobel, Robinson [39,40], Laplace [41], and Laws [10,42]. Convolution filtration of digital images depends on determining derivatives of numerical values of the image with proper selection go color change or gradient change in such a way to achieve adequate sample standard. The primary image is subject to image filtration with the use of masks of  $3 \times 3$ ,  $5 \times 5$ , or  $7 \times 7$  that is applied. In order to apply the Canny filter and to achieve micro-particle edges on image, the original software called "PID system" was used [33].

### 2.4. Binarization

In another step, the image from the Canny filter undergoes binarization obtaining the 1-bit image. Binarization is one of the most important actions of spot image processing [43,44]. In most cases, it precedes image analysis, and it is also very useful in the process of their recognition. Only in case of binary images, it was possible to take the measurements determining the shape coefficient of micro-particles. In order to do this, the Matlab environment with library Hough transform was used [45]. Hough Transform is a very simple method of detecting regular shapes (circles, lines) on the image. This action was tested with ImageJ software [46]. The aim of binarization was a radical reduction of information included in the image as well as extracting shape coordinates of micro-particles.

### 2.5. Image Acquisition

Images of research material samples were obtained using a Nikon D5100 camera with a 16.2-megapixel sensor (CMOS sensor  $23.1 \times 15.4$  mm—DX format), scalytic tent illuminated by visible light (VIS) of warm white color and a color temperature of 6500 Kelvins (K) (Figure 3). In the CMOS matrix, image-setting (exposure to light) and pixel reaction are the same as in the CCD matrix. What differs them is the way of photo-counting and transferring information about luminance that is subject to processing. In the CMOS matrix, each pixel has its own charge—voltage converter, which allows accessing singular point and further transfer information.

Parameters of the research station were calibrated in the following manner: sensitivity of the camera matrix was set at ISO-125, the diaphragm was set at f/8 while exposure time was set at 1/125 sec; length of the prime lens was set to 70 mm, without flash, white balance was set in manual mode. After adequately customizing the parameters to each object subject to imaging and preparing the equipment for image acquisition, we compiled a database in the form of digital images of selected types of fruit powders. For the needs of the research, a previously prepared measurement—research site was selected, which was also used when taking digital images for strawberry powders [10] and rhubarb powders.

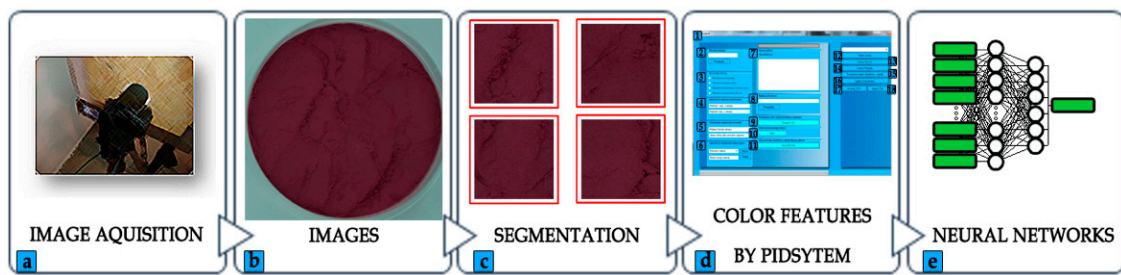


**Figure 3.** Scheme of color features which were extracted from the image to the learning process of Neural Networks: (a)—taking pictures using the research stand; (b)—creating of base of digital photos of chokeberry fruit powders; (c)—image segmentation; (d)—1—image processing module in “PID system”, 2—loading images in the “PID system”, 3—batch image processing selection, 4—determination of image coordinate values (x, y) to be cropped, 5—selection of image format, 6—selection of image pattern to change the name, 7—files list, 8—saving images to the destination directory, 9—extracting color characteristics from images (RGB, YCbCr), 10—approval of the processing process, 11—cleaning the list of objects from the file list window, 12—creating Laws masks, 13—creating Kirch masks, 14—creating Prewitt masks, 15—creating GLCM script to Matlab, 16—creating convolution mask, 17—loading “.csv” file, 18—saving “.csv” file; (e)—learning process ANN.

## 2.6. Principal Component Analysis

One of the methods of factor analysis is the analysis of main components, which, with the use of statistical methods, helps to reduce huge amounts of variables to a few factors, which are not correlated with each other. The PCA analysis was made, whose aim was to reduce training set dimensions [10]. The matrix of correlation of learning sets was also defined, determining the influence of numerical data changeability of image parameters as well as shape compounds [47,48].

## 3. Results and Discussion

### 3.1. Classification

The ANN training process was conducted with network typology type MLP. With a couple of hundred neural networks that were created, the ones characterized by the best classification accuracy were selected, with rather low RMSE. Table 3 shows the results of the training process with sampling of all input variables. The network type MLP was created with 23 input variables, 25 neurons in the hidden layer, and six neurons in the output layer. The MLP 23:23-25-6:1 network was characterized by classification coefficient on the level of 0.92, RMSE = 0.17 and MSE on the level of 0.35. This model presents algorithm BP 50, i.e., the function of learning utilizing algorithm of back-propagating, which in the first stage of learning achieved the lowest level of error in the 50th stage of learning set [49]. Moreover, the conjugate gradient (CG) back-propagation based artificial neural networks for real-time power quality assessment [50]. MLP 23:23-25-6:1 illustrates CG303b, whose aim was to ensure further learning of network during the later stage, as well as to achieve the lowest error causing iteration 303, etc. It is worth paying attention to the fact that the input layer for this model includes 23 image descriptors from model RGB, YCBCR, and H\_S\_B\_L. Dimension reduction of the training set was based on the PCA analysis determining among other things, correlations of input variables (Figure 4) and the analysis of sensitivity for input variables after each process of training was also made for comparison. The MLP 10:10-3-6:1 network is characterized by the worst classification ability, for which the input layer is attributed to the shape coefficient. The shape coefficient was created on the basis of micro-micro-particles distinguished from the image. The influence of applying image filters with the matrix GLCM allowed improving the degree of recognizing the image with colors slightly.

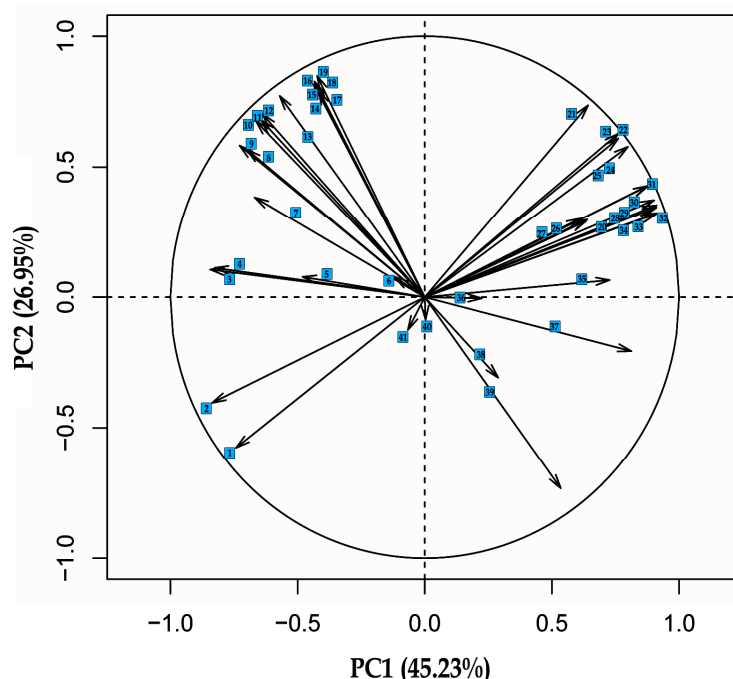


**Figure 4.** PCA of color features: 1—Saturation Mean, 2—Saturation Median, 3—R Std, 4—Saturation Std, 5—Cb Max, 6—HSV Hue, 7—Cb Std, 8—Brightness Std, 9—Luminance Std, 10—Cr Std, 11—Y Std, 12—B Std, 13—G Std, 14—Luminance Max, 15—R Max, 16—Brightness Max, 17—G Max, 18—B Max, 19—Y Max, 20—Luminance Median, 21—G Mean, 22—B Mean, 23—Y Mean, 24—Luminance Mean, 25—Brightness Mean, 26—Y Min, 27—Luminance Min, 28—B Median, 29—G Median, 30—R Median, 31—R Mean, 32—Y Median, 33—Brightness Median, 34—Brightness Min, 35—Cr Median, 36—Cb Median, 37—Cr Mean, 38—Cb Min, 39—Cr Min, 40—Cb Mean, 41—Cr Max [10,33].

Looking at the level of difficulty in recognizing image for chokeberry fruit powders, the subsequent variants of the selection of input variables were taken into consideration. The models of color spaces were separated in input variables, and trials corresponding output variables were divided regarding conditions that influence the process of spray-dried in accordance with Table 1, i.e., temperature: 150 °C—AR\_1, 160 °C—AR\_2 and 170 °C—AR\_3, rotary atomizer speed: 12,000 rpm—AR\_2, 13,000 rpm—AR\_4 and 14,000 rpm—AR\_5 as well as the degree of saccharification of drying carrier (DE): 8—AR\_2 and 14—AR\_6 (Table 4). The network training process showed the influence of selection of color shape model on recognizing chokeberry powders with the same amount of maltodextrin, not recognizing powders on account of the number of carries being used. It turned out that the dominating color space model in recognizing chokeberry powders is YCbCr. The least meaningful discriminants in the process of training were parameters form models HSB and HSL, which led appropriately to retraining the ANN network. The highest classification abilities of network on the level of 0.99 were achieved for MLP 15:15-25-3:1, MLP 15:15-10-2:1 and MLP 12:12-3-2:1. Inlet air temperature, as well as the degree of saccharification of drying carrier (DE) in the process of chokeberry powders drying, had the fundamental meaning in recognizing image regarding a given factor. As a part of comparison, the results of variants of the drying process were collated. Table 4 shows the results with a digital camera. Table 5 shows the results with a selection of variables determining coefficients of micro-particle shape received with electron microscopy. The aim of the experiment was to compare the influence of temperature on spray-drying process, which concerned tests AR\_1, AR\_2, AR\_3 representing neural model MLP 15:15-25-3:1 in relation to the influence of rotational speed of spray disc (the differences in tests) corresponding to neural model with structure MLP 12:12-2-3:1 and MLP 15:15-5-3:1, and in comparison with the influence of the degree crystallization of drying carrier (DE) (differences in tests AR\_2 i AR\_6), which matches neural models MLP 12:12-3-2:1 and MLP 15:15-10-2:1 in Table 4. A lot of parameters have an influence on the properties of powder that is produced; among other things,

the most important parameter in the process of spray drying, apart from the aforementioned factors, is dyeing power. By implication, additional research was done aimed at determining the effectiveness of selecting a model of color space. With PCA analysis, it was possible to reduce variables in a given model of color space (Table 6). In the case of the RGB model validity of variables was determined by 12 parameters from RGB histogram, whereas in the case of YCbCr, these were all parameters from histogram YCbCr. The above information was included in Table 4. The same idea was pointed out in Table 5 on account of particles' shape, but this time not with the use of a camera but with an electron microscope. By comparing Tables 4 and 5, one can notice that the technique of computer image analysis was more effective in recognizing sampling material, i.e., chokeberry powders than SEM technique.

**Table 5.** Results of training process ANN shape coordinates.

Name	MLP 10:10-17-3:1	MLP 10:10-47-2:1	MLP 10:10-30-3:1
Input variables	shape factors	shape factors	shape factors
Output variables	AR_1, AR_2, AR_3	AR_2, AR_6	AR_2, AR_4, AR_5
Training error	0.3285	0.2692	0.3277
Validation error	0.3286	0.2763	0.3296
Testing error	0.3293	0.2820	0.3290
Quality of training	0.4255	0.6555	0.4317
Quality of validation	0.4328	0.6285	0.4273
Quality of testing	0.4064	0.6039	0.4322
Training algorithm	BP50, CG67b	BP50, CG382b	BP50, CG66b
Learning cases	3394	2444	4100
RMSE	0.3288	0.2758	0.3288
MSE	0.5734	0.5252	0.5734
Accuracy	0.4328	0.6285	0.4009

**Table 6.** Eigenvalues by color.

	PC 1	PC 2	PC 3	PC 4	PC 5	PC 6	PC 7	PC 8	PC 9	PC 10
Variance	18.544	11.049	3.519	2.441	1.169	0.936	0.781	0.709	0.461	0.315
% of var.	45.229	26.948	8.582	5.953	2.850	2.283	1.905	1.730	1.125	0.767
Cumulative % of var.	45.229	72.177	80.759	86.712	89.563	91.846	93.751	95.481	96.606	97.373
	PC.11	PC 12	PC 13	PC 14	PC 15	PC 16	PC 17	PC 18	PC 19	PC 20
Variance	0.294	0.191	0.134	0.115	0.100	0.050	0.038	0.031	0.028	0.019
% of var.	0.717	0.466	0.327	0.281	0.245	0.121	0.093	0.076	0.067	0.046
Cumulative % of var.	98.090	98.557	98.884	99.165	99.409	99.530	99.623	99.699	99.767	99.813
	PC.21	PC 22	PC 23	PC 24	PC 25	PC 26	PC 27	PC 28	PC 29	PC 30
Variance	0.018	0.011	0.009	0.008	0.007	0.005	0.005	0.004	0.003	0.002
% of var.	0.044	0.026	0.023	0.019	0.018	0.012	0.012	0.011	0.007	0.006
Cumulative % of var.	99.856	99.882	99.905	99.924	99.942	99.955	99.966	99.977	99.984	99.990

The RMS error level is three times worse while identifying image particles than while identifying image color. Nevertheless, the same relationship is visible in recognizing chokeberry powder classes with a given factor of drying process influencing shape and color. The best ability of classifying the output variables is by determining the degree of saccharification, as well as the changes in the temperature during the process of drying chokeberry powders. It confirmed by laboratory research of physicochemical and bioactive parameters. An increase in inlet air temperature in the process of spray drying has a positive influence on changes of micro-particles, i.e., their sudden growth, and this results in increased efficiency of powder as its looseness, but it has negative influence of bioactive properties [5]. In the case of the degree of saccharification of the carrier (DE), substantial statistical changes were noted down in the case of particle shape and powders looseness [5]. The worst ability to classify in case of variation of rotary atomizer speed is also confirmed with a quality assessment conducted in the laboratory. In the case of this given variable form most marked parameters, major statistical quality changes were not noted down [5].

### 3.2. Results of Principal Component Analysis

The PCA analysis was made with a training set characterized by a color space model with 41 input variables. The set was reduced to the minimum possible set of numerical data of color space models (Figure 4). Tables 6 and 7 present proprietary values for training sets, on the basis of which main components of PCA, as well as vector effects, were illustrated (see Figures 1 and 2). The aforementioned set with variables was reduced, eliminating input variables, such as Hue, R Max, R Std, Y Min, Y Std, Cb Max, Cb Median, Cb Min, Cb Std, Cr Max, all Brightness, Luminance Median, Min, Std. On the basis of the PCA analysis that was made, ANN was received. The training set basis on shape coordinates with 13 input variables was reduced to 10 input variables. As a result of the reduction, MinFerret, Feret, as well as Area was rejected.

**Table 7.** Eigenvalues by shape factors.

	PC1	PC2	PC3	PC4	PC5	PC6	PC7	PC8	PC9	PC10
Variance	7.530	2.954	1.233	0.478	0.243	0.202	0.173	0.089	0.043	0.037
% of var.	57.926	22.720	9.488	3.674	1.868	1.551	1.332	0.682	0.334	0.281
Cumulative % of var.	57.926	80.646	90.134	93.808	95.675	97.227	98.558	99.240	99.574	99.856

In the second phase, the level of correlation between variables was analyzed. Strong correlation in the training set of color models occurred between variables Y Mean and Y Median, and the correlation coefficient was on the level of 0.951. Equally strongly correlated negative results were received between Y Max and Cr Min and amounted to  $r^2 = 0.913$ . In the RGB model, the strongest correlation is between variables B Max and G Max, on the level of  $r^2 = 0.996$ . Comparing parameters between the models YCbCr and RGB, a strong correlation is between the aforementioned variables, i.e., Y Max and B Max on the level of 0.999. However, a strong negative correlation is between variables G Max and Cr Min on the level of 0.932.

In case of data variations between parameters in training set of shape coefficient, a strong correlation occurs between Feret and aspect ratio (AR) coefficients on the level of  $r^2 = 0.951$  and a strong negative correlation of the aforementioned coefficient form Round on the level of  $r^2 = 0.815$  (Figure 5).

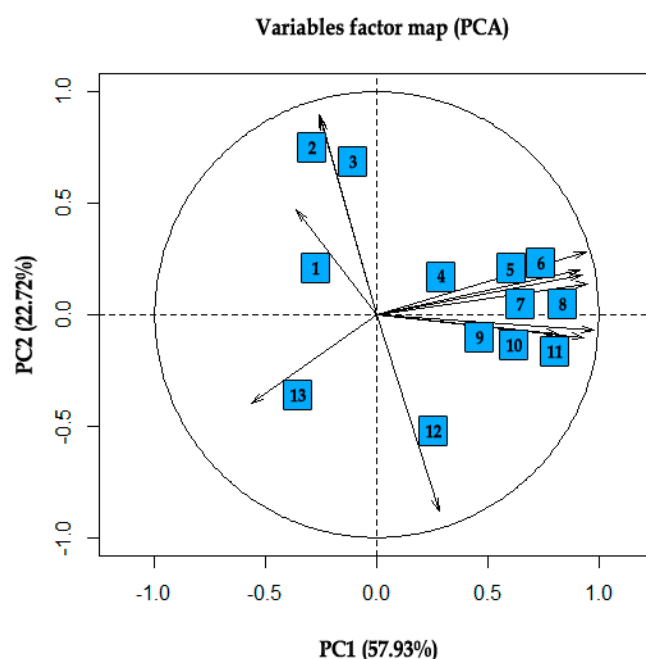


**Figure 5.** PCA of shape factors: 1—Malinowska factor 2—aspect ratio (AR), 3—Feret factor, 4—Feret diameter X, 5—height, 6—width, 7—W2\_circumference 2, 8—height, 9—W1\_circumference 1, 10—Feret diameter Y, 11—Area, 12—Round, 13—Solidity [10,46].

#### 4. Conclusions

Utilization of the two vision techniques with a digital camera and scanning microscope found out that more efficient recognition of quality classes of stay dried chokeberry juice occurs when using color ratio. The best color space model having an influence on the ability to recognize digital images turned out to be the model YCbCr. On the basis of the PCA analysis, it was pointed out that the strongest correlation occurs for the component Y of the model YCbCr. Neural models, in which shape coefficients are included, demonstrated, like in the case of strawberry micro-particles [10], that the efficiency of recognizing micro-particles is dependent on their diameter. On the basis of the PCA analysis, the strongest correlation occurs between Feret coordinates and other input variables determining shape coordinates. Size reduction of input variables in the PCA analysis, improved efficiency of recognizing the image of digital pictures as well as SEM, and at the same time improving the level of trying neural models.

The selection of input variables on account of the selection of factors in the process of drying substantially responds to the improvement of the abilities of the training network. The best-classified parameters in the process of drying were received during recognizing the degree of saccharification (DE) of carrier and different temperatures of drying between trials. It is confirmed by laboratory research of physicochemical and bioactive parameters that were done. An increase in inlet air temperature in the process of spray drying has a positive influence on changes in micro-particles, i.e., their sudden growth, and this results in increased efficiency of fruit powders as well as its looseness; however, it has a negative influence on bioactive properties [5]. In case of the degree of saccharification of the carrier (DE), substantial statistical changes were noted down regarding the size of particles and powder looseness [5]. The worst classification abilities in case variations of rotary atomizer speed are also confirmed by the quality assessment conducted in the laboratory. In the case of this variable for most marked parameters, substantial statistical changes in quality were not detected [5].

The biggest classification abilities were reached by network typology, the Multi-Layer Perceptron. Neural models, which were characterized by the highest quality of degree classification on the level of 0.99, were reached by MLP networks with structure. 15:15-25-3:1, 12:12-3-2:1 and 15:15-10-2:1.

**Author Contributions:** Conceptualization, K.P. and J.G.; methodology, K.P. and K.K.; software, K.P.; validation, K.P.; formal analysis, J.G. and M.R.; investigation, J.P.; resources, J.P.; data curation, J.G.; writing—original draft preparation, M.R.; writing—review and editing, K.K. and J.G.; visualization, K.K.; supervision, E.D.; project administration, Ł.G.

**Funding:** The authors are grateful for financial support provided by the Poznań University of Life Sciences, Poland, within the framework of fund no.506.752.03.00.

**Conflicts of Interest:** The authors declare no conflict of interest.

#### References

1. Hellström, J.K.; Shikov, A.N.; Makarova, M.N.; Pihlanto, A.M.; Pozharitskaya, O.N.; Ryhänen, E.L.; Kivijärvi, P.; Makarov, V.G.; Mattila, P.H. Blood pressure-lowering properties of chokeberry (*Aronia mitchurinii*, var. Viking). *J. Funct. Foods* **2010**, *2*, 163–169. [[CrossRef](#)]
2. Wawer, I. *The Power of Nature, Aronia Melanocarpa*; Mae's Health and Wellness LCC: Omaha, NE, USA, 2010.
3. Bermúdez-Soto, M.J.; Larrosa, M.; Garcia-Cantalejo, J.M.; Espín, J.C.; Tomás-Barberan, F.A.; García-Conesa, M.T. Up-regulation of tumor suppressor carcinoembryonic antigen-related cell adhesion molecule 1 in human colon cancer Caco-2 cells following repetitive exposure to dietary levels of a polyphenol-rich chokeberry juice. *J. Nutr. Biochem.* **2007**, *18*, 259–271. [[CrossRef](#)] [[PubMed](#)]
4. Kulling, S.; Rawel, H. Chokeberry (*Aronia melanocarpa*)—A Review on the Characteristic Components and Potential Health Effects. *Planta Med.* **2008**, *74*, 1625–1634. [[CrossRef](#)] [[PubMed](#)]
5. Gawalek, J.; Domian, E.; Ryniecki, A.; Bakier, S. Effects of the spray drying conditions of chokeberry (*Aronia melanocarpa* L.) juice concentrate on the physicochemical properties of powders. *Int. J. Food Sci. Technol.* **2017**, *52*, 1933–1941. [[CrossRef](#)]

6. Krenn, L.; Steitz, M.; Schlicht, C.; Kurth, H.; Gaedcke, F. Anthocyanin- and proanthocyanidin-rich extracts of berries in food supplements—Analysis with problems. *Die Pharm. Int. J. Pharm. Sci.* **2007**, *62*, 803–812.
7. Mazza, G. *Anthocyanins in Fruits, Vegetables, and Grains*; Mazza, G., Miniati, E., Eds.; CRC Press: Boca Raton, FL, USA, 2018; ISBN 9781351069700.
8. Šnebergrová, J.; Čížková, H.; Neradová, E.; Kapci, B.; Voldřich, M. Variability of characteristic components of aronia. *Czech J. Food Sci.* **2014**, *32*, 25–30. [[CrossRef](#)]
9. Jeppsson, N. The effects of fertilizer rate on vegetative growth, yield and fruit quality, with special respect to pigments, in black chokeberry (*Aronia melanocarpa*) cv. “Viking”. *Sci. Hortic.* **2000**, *83*, 127–137. [[CrossRef](#)]
10. Przybył, K.; Gawałek, J.; Koszela, K.; Wawrzyniak, J.; Gierz, L. Artificial neural networks and electron microscopy to evaluate the quality of fruit and vegetable spray-dried powders. Case study: Strawberry powder. *Comput. Electron. Agric.* **2018**, *155*, 314–323. [[CrossRef](#)]
11. Russo, P.; Adiletta, G.; Di Matteo, M. The influence of drying air temperature on the physical properties of dried and rehydrated eggplant. *Food Bioprod. Process.* **2013**, *91*, 249–256. [[CrossRef](#)]
12. Muzaffar, K.; Nayik, G.A.; Kumar, P. Stickiness Problem Associated with Spray Drying of Sugar and Acid Rich Foods: A Mini Review. *J. Nutr. Food Sci.* **2015**, *S12*, 3. [[CrossRef](#)]
13. Bhandari, B.; Bansal, N.; Zhang, M.; Schuck, P. *Handbook of Food Powders: Processes and Properties*; Elsevier: Amsterdam, The Netherlands, 2013; ISBN 9780857098672.
14. Phisut, N. Spray drying technique of fruit juice powder: Some factors influencing the properties of product. *Int. Food Res. J.* **2012**, *19*, 1297–1306.
15. Gharsallaoui, A.; Roudaut, G.; Chambin, O.; Voilley, A.; Saurel, R. Applications of spray-drying in microencapsulation of food ingredients: An overview. *Food Res. Int.* **2007**, *40*, 1107–1121. [[CrossRef](#)]
16. Mishra, P.; Brahma, A.; Seth, D. Physicochemical, functionality and storage stability of hog plum (*Spondia pinnata*) juice powder produced by spray drying. *J. Food Sci. Technol.* **2017**, *54*, 1052–1061. [[CrossRef](#)] [[PubMed](#)]
17. Chegini, G.R.; Ghobadian, B. Spray Dryer Parameters for Fruit Juice Drying. *World J. Agric. Sci.* **2007**, *3*, 230–236.
18. Fitzpatrick, J.J.; Barringer, S.A.; Iqbal, T. Flow property measurement of food powders and sensitivity of Jenike’s hopper design methodology to the measured values. *J. Food Eng.* **2004**, *61*, 399–405. [[CrossRef](#)]
19. Santomaso, A.; Lazzaro, P.; Canu, P. Powder flowability and density ratios: The impact of granules packing. *Chem. Eng. Sci.* **2003**, *58*, 2857–2874. [[CrossRef](#)]
20. Gawałek, J.; Bartczak, P. Effect of red beet juice spray drying conditions on selected properties of produced powder. *Food Sci. Technol. Qual.* **2014**, *2*, 164–174. [[CrossRef](#)]
21. Chaudhuri, B.; Mehrotra, A.; Muzzio, F.J.; Tomassone, M.S. Cohesive effects in powder mixing in a tumbling blender. *Powder Technol.* **2006**, *165*, 105–114. [[CrossRef](#)]
22. Landillon, V.; Cassan, D.; Morel, M.H.; Cuq, B. Flowability, cohesive, and granulation properties of wheat powders. *J. Food Eng.* **2008**, *86*, 178–193. [[CrossRef](#)]
23. Szulc, K.; Lenart, A. Cohesion properties of selected food powders. *Agric. Eng.* **2009**, 169–175. Available online: [http://yadda.icm.edu.pl/yadda/element/bwmeta1.element.baztech-article-BAR0-0045-0061/c/httpir\\_ptir\\_orgartykulypl111ir1112478pl.pdf](http://yadda.icm.edu.pl/yadda/element/bwmeta1.element.baztech-article-BAR0-0045-0061/c/httpir_ptir_orgartykulypl111ir1112478pl.pdf) (accessed on 10 October 2019).
24. Shishir, M.R.I.; Chen, W. Trends of spray drying: A critical review on drying of fruit and vegetable juices. *Trends Food Sci. Technol.* **2017**, *65*, 49–67. [[CrossRef](#)]
25. Gómez-Carracedo, M.P.; Andrade, J.M.; Carrera, G.V.S.M.; Aires-de-Sousa, J.; Carlosena, A.; Prada, D. Combining Kohonen neural networks and variable selection by classification trees to cluster road soil samples. *Chemom. Intell. Lab. Syst.* **2010**, *102*, 20–34. [[CrossRef](#)]
26. Boniecki, P.; Piekarska-Boniecka, H.; Koszela, K.; Zaborowicz, M.; Przybył, K.; Wojcieszak, D.; Zbytek, Z.; Ludwiczak, A.; Przybylak, A.; Lewicki, A. Neural Classifier in the Estimation Process of Maturity of Selected Varieties of Apples. In Proceedings of the Seventh International Conference on Digital Image Processing (ICDIP 2015), Los Angeles, CA, USA, 9–10 April 2015; Volume 9631.
27. Koszela, K.; Przybył, J.; Kujawa, S.; Kozłowski, R.J.; Przybył, K.; Niedbała, G.; Idziaszek, P.; Boniecki, P.; Zaborowicz, M. IT system for the identification and classification of soil valuation classes. In Proceedings of the SPIE—The International Society for Optical Engineering, Chengdu, China, 20–22 May 2016; Volume 10033.

28. Borah, S.; Hines, E.L.; Bhuyan, M. Wavelet transform based image texture analysis for size estimation applied to the sorting of tea granules. *J. Food Eng.* **2007**, *79*, 629–639. [[CrossRef](#)]
29. Boniecki, P.; Nowakowski, K.; Tomczak, R. Neural Networks Type MLP in the Process of Identification Chosen Varieties of Maize. *Proc. SPIE Int. Soc. Opt. Eng.* **2011**, *8009*, 11–13.
30. Nowakowski, K.; Boniecki, P.; Tomczak, R.J.; Kujawa, S.; Raba, B. *Identification of Malting Barley Varieties Using Computer Image Analysis and Artificial Neural Networks*; Othman, M., Senthilkumar, S., Yi, X., Eds.; International Society for Optics and Photonics: Kaula Lumpur, Malaysia, 2012; p. 833425.
31. Przybył, K.; Zaborowicz, M.; Koszela, K.; Boniecki, P.; Mueller, W.; Raba, B.; Lewicki, A. Organoleptic damage classification of potatoes with the use of image analysis in production process. In Proceedings of the SPIE—The International Society for Optical Engineering, Athens, Greece, 11 May 2014; Volume 9159.
32. Tadeusiewicz, R. Neural networks: A comprehensive foundation. *Control Eng. Pract.* **1995**, *3*, 746–747. [[CrossRef](#)]
33. Przybył, K.; Ryniecki, A.; Niedbała, G.; Mueller, W.; Boniecki, P.; Zaborowicz, M.; Koszela, K.; Kujawa, S.; Kozłowski, R.J. Software supporting definition and extraction of the quality parameters of potatoes by using image analysis. In Proceedings of the SPIE—The International Society for Optical Engineering, Chengu, China, 20–22 May 2016; Volume 10033.
34. Manickavasagan, A.; Al-Mezeini, N.K.; Al-Shekaili, H.N. [RGB] color imaging technique for grading of dates. *Sci. Hortic.* **2014**, *175*, 87–94. [[CrossRef](#)]
35. García-Mateos, G.; Hernández-Hernández, J.L.; Escarabajal-Henarejos, D.; Jaén-Terrones, S.; Molina-Martínez, J.M. Study and comparison of color models for automatic image analysis in irrigation management applications. *Agric. Water Manag.* **2015**, *151*, 158–166. [[CrossRef](#)]
36. Brancati, N.; De Pietro, G.; Frucci, M.; Gallo, L. Human skin detection through correlation rules between the YCb and YCr subspaces based on dynamic color clustering. *Comput. Vis. Image Underst.* **2017**, *155*, 33–42. [[CrossRef](#)]
37. Canny, J. A Computational Approach to Edge Detection. *IEEE Trans. Pattern Anal. Mach. Intell.* **1986**, *6*, 679–698. [[CrossRef](#)]
38. Sengupta, S.; Lee, W.S. Identification and determination of the number of immature green citrus fruit in a canopy under different ambient light conditions. *Biosyst. Eng.* **2014**, *117*, 51–61. [[CrossRef](#)]
39. Muthukrishnan, R.; Radha, M. Edge Detection Techniques for Image Segmentation. *Int. J. Comput. Sci. Inf. Technol.* **2012**, *3*, 259. [[CrossRef](#)]
40. Okoń, P.; Kozowski, R.J.; Zaborowicz, M.; Górna, K.; Ludwiczak, A.; Slószarz, P.; Janiszewski, P.; Strzełiński, P.; Jurek, P.; Koszela, K.; et al. Possibilities for the use of edge detection algorithms in the analysis of images of oilseed rape leaves. In Proceedings of the SPIE—The International Society for Optical Engineering, Chengu, China, 20–22 May 2016; Volume 10033.
41. Radke, R.J.; Andra, S.; Al-Kofahi, O.; Roysam, B. Image change detection algorithms: A systematic survey. *IEEE Trans. Image Process.* **2005**, *14*, 294–307. [[CrossRef](#)] [[PubMed](#)]
42. Laws, K.I. Rapid Texture Identification. In *Image Processing for Missile Guidance*; International Society for Optics and Photonics: San Diego, CA, USA, 1980; Volume 238, pp. 376–381.
43. Chaki, N.; Shaikh, S.H.; Saeed, K. A Comprehensive Survey on Image Binarization Techniques. In *Exploring Image Binarization Techniques*; Springer: New Delhi, India, 2014; pp. 5–15. ISBN 978-81-322-1907-1.
44. Lu, D.; Huang, X.; Sui, L. Binarization of degraded document images based on contrast enhancement. *Int. J. Doc. Anal. Recognit.* **2018**, *21*, 123–135. [[CrossRef](#)]
45. Matas, J.; Galambos, C.; Kittler, J. Robust detection of lines using the progressive probabilistic hough transform. *Comput. Vis. Image Underst.* **2000**, *78*, 119–137. [[CrossRef](#)]
46. Ferreira, T.; Rasband, W. ImageJ User Guide IJ 1.46r. IJ 1.46r 185. Available online: <https://imagej.nih.gov/ij/docs/guide/user-guide.pdf> (accessed on 10 October 2019).
47. Ghosh, D.; Chattopadhyay, P. Application of principal component analysis (PCA) as a sensory assessment tool for fermented food products. *J. Food Sci. Technol.* **2012**, *49*, 328–334. [[CrossRef](#)] [[PubMed](#)]
48. Dharmasena, L.S.; Zeephongsekul, P. A new process capability index for multiple quality characteristics based on principal components. *Int. J. Prod. Res.* **2016**, *54*, 4617–4633. [[CrossRef](#)]

49. Burks, T.F.; Shearer, S.A.; Heath, J.R.; Donohue, K.D. Evaluation of Neural-network Classifiers for Weed Species Discrimination. *Biosyst. Eng.* **2005**, *91*, 293–304. [[CrossRef](#)]
50. Khadse, C.B.; Chaudhari, M.A.; Borghate, V.B. Conjugate gradient back-propagation based artificial neural network for real time power quality assessment. *Int. J. Electr. Power Energy Syst.* **2016**, *82*, 197–206. [[CrossRef](#)]



© 2019 by the authors. Licensee MDPI, Basel, Switzerland. This article is an open access article distributed under the terms and conditions of the Creative Commons Attribution (CC BY) license (<http://creativecommons.org/licenses/by/4.0/>).